

## High- $\beta$ Equilibria of Drift-Optimized Compact Stellarators

A. S. Ware,<sup>1</sup> S. P. Hirshman,<sup>2</sup> D. A. Spong,<sup>2</sup> L. A. Berry,<sup>2</sup> A. J. Deisher,<sup>1</sup> G. Y. Fu,<sup>3</sup> J. F. Lyon,<sup>2</sup> and R. Sanchez<sup>4</sup>

<sup>1</sup>University of Montana–Missoula, Missoula, Montana 59812

<sup>2</sup>Oak Ridge National Laboratory, Oak Ridge, Tennessee 37831

<sup>3</sup>Princeton Plasma Physics Laboratory, Princeton, New Jersey 08543

<sup>4</sup>Universidad Carlos III de Madrid, Madrid, Spain

(Received 12 February 2002; published 30 August 2002)

Compact stellarator configurations have been obtained with good neoclassical confinement that are stable to both pressure- and current-driven modes for high values of  $\beta$ . These configurations are drift-optimized tokamak-stellarator hybrids with a high-shear tokamak-like rotational transform profile and  $|B|$  that is approximately poloidally symmetric. The bootstrap current is consistent with the required equilibrium current and, while larger than that in existing stellarators, is typically only a small fraction ( $1/3 - 1/5$ ) of that in an equivalent tokamak. These configurations have strong magnetic wells and consequently high interchange stability  $\beta$  limits up to  $\beta = 23\%$ . Because of the reduced bootstrap current, these configurations are stable to low- $n$  ideal MHD kink modes with no wall stabilization for values of  $\beta$  ( $\sim 7\% - 11\%$ ) significantly larger than in an equivalent advanced tokamak.

DOI: 10.1103/PhysRevLett.89.125003

PACS numbers: 52.55.Hc, 52.55.Fa, 52.55.Tn

Interest in compact stellarators with aspect ratios  $A = \langle R \rangle / \langle a \rangle$  in the range  $2 < A < 4$  is motivated by the desire to realize an economically sized, high-power-density fusion reactor with little or no recirculating power and freedom from discharge-terminating disruptions. Here  $\langle R \rangle$  and  $\langle a \rangle$  are the average major and minor radii, respectively, of these noncircular, nonaxisymmetric plasmas. Lower values of  $A$  are expected to lead to higher  $\beta$  limits provided regions of locally unfavorable curvature can be avoided. High  $\beta$  is needed to achieve feasible magnetic field strengths at the coils of a stellarator reactor. However, magnetic drifts are enhanced at low  $A$ . This, in combination with strong departures from geometric symmetry, leads to enhanced neoclassical transport. Here,  $\beta = 2\mu_0 \langle p \rangle / \langle B^2 \rangle$  is the normalized volume-averaged plasma pressure.

Drift optimization [1], which is a technique for aligning bounce-averaged particle drift surfaces with magnetic surfaces, has been successfully applied to suppress this deterioration of particle and energy confinement in compact devices [2]. This approach complements the use of quasisymmetry, which was applied to the designs of the Helically Symmetric Stellarator [3] and the proposed National Compact Stellarator Experiment [4]. Spong *et al.* [5] have analyzed the impact of drift optimization on neoclassical transport, primarily focusing on properties of a compact, lower- $\beta$  stellarator with low-bootstrap current and a stellaratorlike rotational transform ( $\iota \sim 1/\text{pitch} = 1/q$ ) profile with low shear that is relatively invariant to changes in  $\beta$ . Shear is the radial change of  $\iota$  with radius. Spong *et al.* also noted the existence of a new type of higher- $\beta$ , compact stellarator. Here, we describe for the first time the complete physics properties of the higher- $\beta$  configurations. These configurations are tokamak-stellarator hybrids with a higher (self-consistent) bootstrap current and  $|B|$  exhibiting approxi-

mate quasipoloidal symmetry (qps). This symmetry is defined by  $d|B|/d\theta_B \sim 0$ , where  $\theta_B$  is the poloidal Boozer flux angle [6]. Figure 1 shows the last closed flux surfaces for two qps configurations: QPS3, with three field periods ( $N = 3$ ) and high  $\beta \sim 15\%$ , and QPS2, with two field periods ( $N = 2$ ) and moderate  $\beta \sim 5\%$ . The colors indicate contours of constant  $|B|$ . The new configurations have a high-shear  $\iota$  profile which decreases with plasma minor radius (as in a conventional tokamak) and for which the calculated neoclassical cross-field transport decreases with  $\beta$  because  $|B|$  more closely approximates poloidal symmetry. The nonaxisymmetric Fourier components ( $n \neq 0$ ) of  $|B|$  result in a reduced bootstrap current that is only  $1/5 - 1/3$  that of an equivalent tokamak (a torus with the same axisymmetric boundary Fourier components and rotational transform as this qps configuration). The lower current results in MHD stability  $\beta$  limits that are higher than those for the equivalent tokamak:  $\beta > 20\%$  for Mercier and ballooning stability and  $\beta \sim 11\%$  for vertical and kink stability without a conducting wall.

Unlike classical stellarators, or even some of the quasisymmetric stellarators previously considered, these high- $\beta$  qps configurations are distinguished by a relatively small external rotational transform arising from coils (typically,  $\iota_{\text{coils}} \sim 0.05 - 0.10$ ). As in a tokamak, the dominant contribution to the rotational transform (away from the plasma edge, at least) is produced by the plasma current. Hence these are stellarator-tokamak hybrid configurations. For the QPS3 configuration in Fig. 1(a),  $\iota$  varies monotonically from 0.4 on axis to 0.1 at the edge, with approximately half of the edge transform due to currents in the external coils. Note that this profile avoids the  $\iota = 1/2$  and other low-order resonances (where  $\iota = M/N$ ), so internal disruptions should be suppressed. The shear is large so that neoclassical tearing-mode

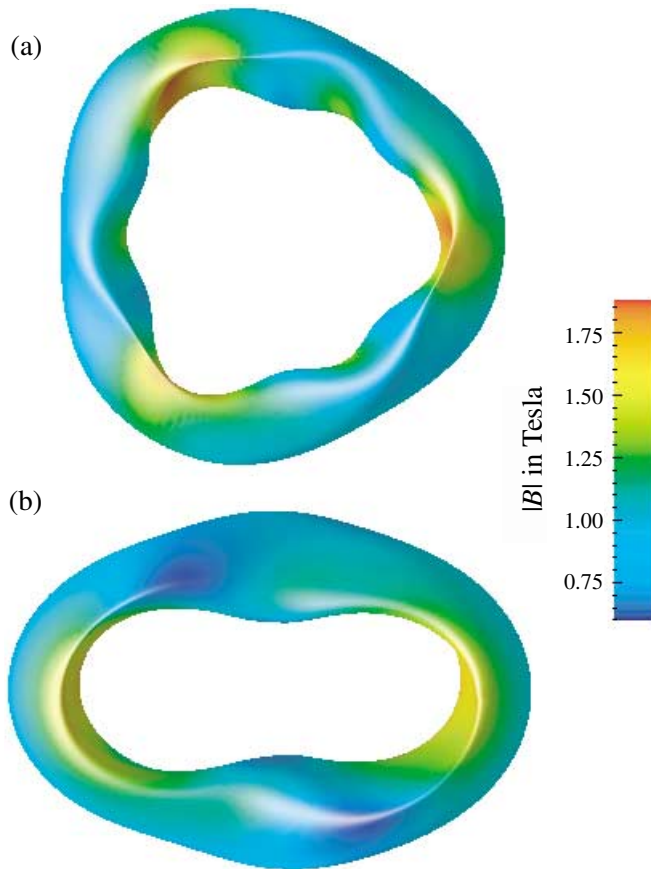


FIG. 1 (color). Last closed flux surface for (a) QPS3, with three field periods,  $A = 3.7$ ,  $\beta = 15\%$ , and (b) QPS2, with two field periods,  $A = 2.7$ ,  $\beta = 5\%$ . Color indicates the variation in  $|B|$ .

islands should also be suppressed, although not completely stabilized.

The main role of the external stellarator coils in these qps configurations is to substantially reduce (but not eliminate) the bootstrap current. The neoclassical current was computed using an analytic model [7], which was incorporated into an iterative nonlinear stellarator optimization code [5]. The QPS2 and QPS3 configurations were optimized for consistency of the equilibrium and bootstrap currents so that the required equilibrium plasma current was composed entirely of the bootstrap current associated with the pressure and  $\iota$  profiles. As previously noted, the bootstrap currents for these cases are lower than that in an equivalent tokamak. Alternatively, the bootstrap current in such a tokamak would be too large to be consistent with these values of  $\iota$  and  $\beta$ . Figure 2 shows the profiles of the equilibrium current (green squares), the computed bootstrap current (blue circles), and the bootstrap current in an equivalent tokamak (red diamonds) as a function of the normalized toroidal flux variable  $s \sim (r/a)^2$  for the QPS3 configuration. The reduction in the bootstrap current is due to the approximate quasipoloidal symmetry of  $|B|$ . Figure 3

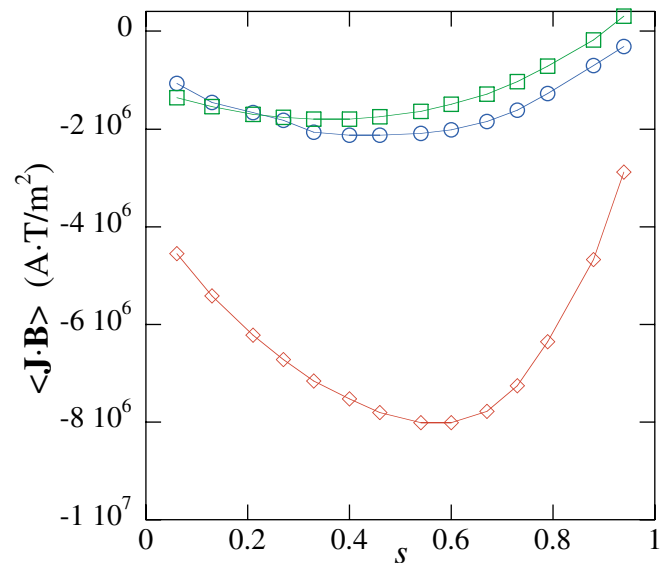


FIG. 2 (color). Profiles of  $\langle \mathbf{J} \cdot \mathbf{B} \rangle$  for QPS3 shown in Fig. 1(a). Shown are the equilibrium current (green squares), bootstrap current (blue circles), and bootstrap current in an equivalent tokamak (red diamonds). The currents are antiparallel to the magnetic field. Thus, the magnitude of the current decreases toward the top.

shows contours of  $|B|$  in magnetic flux coordinates for QPS3 on the flux surface  $\rho = \sqrt{s} = 0.75$ . While the poloidal variation of  $|B|$  is small, the components that break the qps are non-negligible. Exact qps would reduce the bootstrap current by a factor  $\sim \iota/N$  (which is comparable to what is computed numerically). This differs from the near cancellation of toroidal and helical components of current in Wendelstein 7-X [1] and the low-bootstrap-current, quasisymmetric stellarators [5]. Self-consistent bootstrap current profiles have been obtained for plasmas in the range  $2\% < \beta < 23\%$ .

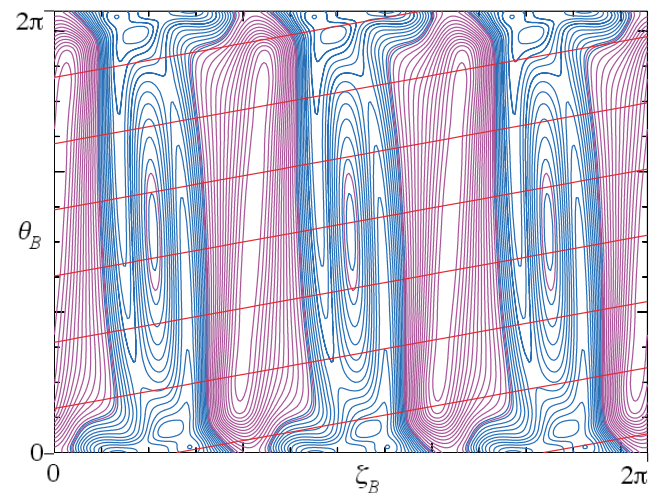


FIG. 3 (color). Contours of  $|B|$  in Boozer coordinates on the  $\rho = 0.75$  flux surface for QPS3 shown in Fig. 1(a). Blue contours indicate  $|B| < 1$  T, purple contours indicate  $|B| > 1$  T, and red lines indicate the direction of magnetic field lines.

The bootstrap current is proportional to the Onsager transport coefficient ( $L_{31}$ ), which is shown for the QPS3 configuration in Fig. 4 as a function of  $\nu/\nu$  for several values of  $\beta$  (but with fixed shape and rotational transform profile). Here,  $\nu$  is the collision frequency and  $\nu$  is the particle speed. A neoclassical transport code [8] was used to solve the drift kinetic equation in magnetic flux coordinates and stellarator geometry. The computed coefficient  $L_{31}$  decreases as  $\beta$  increases. This results in the bootstrap current, which is proportional to the product of  $L_{31}$  and  $\beta$ , becoming nearly independent of  $\beta$  at higher values of  $\beta$ . This is a unique form of configurational invariance: the nonzero bootstrap current and, hence, the  $\iota$  profile remain nearly constant as  $\beta$  increases. Therefore, new low-order rational resonant surfaces do *not* enter the plasma as  $\beta$  increases (so the magnetic surfaces should be configurationally robust), and a simple vertical field should suffice to compensate for outward radial shifts of the flux surfaces due to the Pfirsch-Schlüter current.

The presence of a finite bootstrap current distinguishes these qps configurations from previous compact stellarators which have very low-bootstrap current and results in reductions of both the helical curvature and the connection length. Both of these effects contribute to the higher ballooning stability  $\beta$  limits that are computationally observed. Infinite- $n$  ballooning mode stability was analyzed using the numerically efficient ballooning code COBRA [9], which was also incorporated into the stellarator optimization code. By optimizing the shape of the

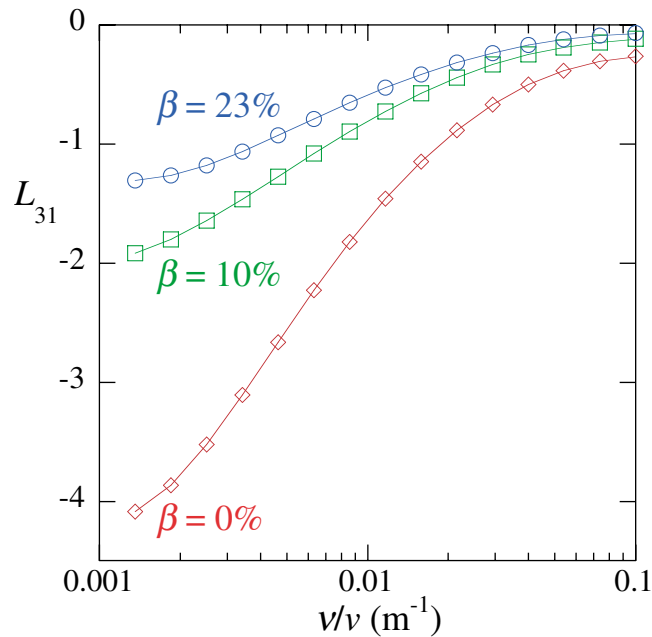


FIG. 4 (color).  $L_{31}$  bootstrap transport coefficient for QPS3 as a function of ion collisional frequency parameter for three values of  $\beta$ .

last closed magnetic flux surface, together with the pressure profile, for targeted values of  $\beta$ , we obtained ballooning-stable configurations with self-consistent bootstrap current for plasmas in the range  $2\% < \beta < 23\%$ . For the QPS3 high- $\beta$  configurations, decreasing  $\beta$  with fixed shape and  $\iota$  profile resulted in ballooning-unstable configurations. Figure 5 shows ballooning growth rates across the minor radius of QPS3 as  $\beta$  is varied. As  $\beta$  is lowered to 13%, a single surface near the edge becomes unstable. The edge region of instability broadens, and the maximum growth rate becomes larger as  $\beta$  is lowered to 9%. As  $\beta$  is further lowered to 3%, the edge region of instability increases, but the peak growth rate decreases. The plasma finally becomes ballooning stable again for  $\beta < 0.5\%$ . This stability behavior as a function of  $\beta$  indicates that these plasmas are in the second-stable ballooning regime for  $\beta > 13\%$ . We note that relatively small shape and profile modifications can produce stable plasmas at all values of  $\beta < 23\%$  for QPS3. Future work on the QPS3 configurations will examine the unresolved issue of accessing high- $\beta$  regimes from low  $\beta$ .

These configurations have good Mercier (local interchange) stability properties resulting from a magnetic well over the entire plasma cross section, with the exception of a few isolated resonances where  $\iota$  takes on low-order rational values. The resulting localized interchange instabilities could lead to lower  $\beta$  values if they occur near the plasma edge and if they proliferate over a range of radii. The QPS3 ( $\beta = 15\%$ ) configuration is Mercier stable except near the  $\iota = 1/5$  and  $\iota = 5/12$  resonances, which occur well inside the plasma. The QPS2 ( $\beta = 5\%$ )

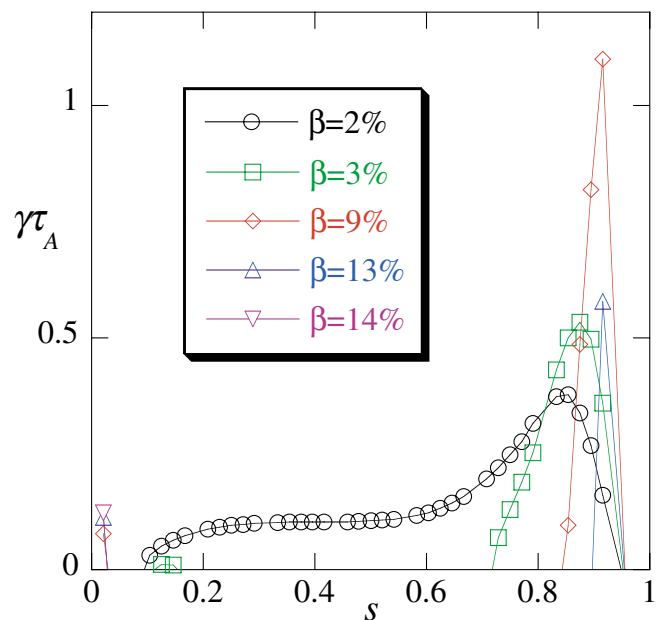


FIG. 5 (color). Ballooning growth rate as a function of  $\beta$  for QPS3.

configuration is Mercier stable except near the  $\iota = 3/8$  resonance.

The presence of a nonzero net plasma current in these compact stellarators makes them potentially susceptible to vertical and kink modes. Stability to these modes was assessed using the Terpsichore code [10] after completion of the other optimizations. In spite of its nonzero plasma current and high  $\beta \sim 15\%$ , the QPS3 configuration was stable to vertical modes and only weakly unstable to an external kink mode (with normalized growth rate  $\gamma\tau_A \sim 2 \times 10^{-2}$ , where  $\tau_A$  is the Alfvén time). Keeping the same shape but scaling  $\beta$  down to  $\sim 11\%$  (keeping  $\iota$  fixed) completely stabilized the kink mode. At this value of  $\beta$ , the Troyon factor,  $\beta_N \equiv \beta(\%)[\langle a(m) \rangle B(T)/I(\text{MA})]$ , reaches a value of  $\beta_N = 19$ , which is significantly larger than  $\beta_N \sim 3$  for kink stability in an equivalent tokamak with no wall stabilization. This stability at high  $\beta$  to the most deleterious modes (for tokamaks) is achieved by the nonaxisymmetric components in  $|B|$ , which reduce the self-consistent bootstrap current to a small fraction of that for a tokamak with a similar  $\iota$  and shape.

The QPS2 configuration is computed to have a lower stability  $\beta$  threshold for the vertical mode than QPS3. However, by either increasing the fraction of external rotational transform or reducing the axisymmetric elongation [11], related configurations that were stable to the vertical mode up to  $\beta \sim 5\%$  could be achieved. Stabilization of these low- $n$  macroscopic modes should also be possible, either through current profile tailoring (reducing the pressure gradient, and hence the bootstrap current, near the plasma edge) or through dynamic feedback provided by suitable external coils, as is done for shaped tokamaks.

Neoclassical confinement is a concern for compact stellarator configurations because of the residual non-symmetry of  $|B|$ . Using both drift-orbit and enhanced quasipoloidal symmetry optimization targets has led to the present configurations, which have adequate levels of neoclassical confinement. Neoclassical ion and electron confinement times were calculated using a Monte Carlo approach [5]. For a QPS3 configuration scaled down to the size and field strength ( $\langle R \rangle = 0.86$  m,  $\langle B \rangle = 1$  T) of a near-term experiment, the predicted global neoclassical energy confinement time ( $\tau_{E_{\text{neoc}}}$ ) is 14 ms for a low-collision-frequency, hot-electron plasma and 58 ms for a moderate-collision-frequency plasma with equal ion and electron temperatures. A comparison of these times with the confinement time predicted by the ISS95 empirical scaling law [12] yields  $\tau_{E_{\text{neoc}}}/\tau_{E_{\text{ISS95}}} = 1.4\text{--}3.6$  for expected values of the radial electric field. Under these conditions, the neoclassical losses are tolerable in the sense that anomalous processes should dominate the thermal transport. A kinetic transport code [8] was used within the iterative stellarator optimization process to further improve  $\tau_{E_{\text{neoc}}}$  for these plasmas, after a promising region of configurations had been identified. A factor of 2

increase in  $\tau_{E_{\text{neoc}}}$  was obtained by minimizing the local radial particle and energy transport at several surfaces without sacrificing ballooning and kink stability.

An attractive feature of these configurations is that as  $\beta$  increases, the alignment of particle drift and magnetic flux surfaces improves, as in Wendelstein 7-X [1]. The previously mentioned configurational invariance that is achieved in these devices results from the improved degree of qps with increasing  $\beta$ . High  $\beta$  also results in a diamagnetic depression (magnetic well) of the  $|B|_{0,0}$  component of the magnetic field. The resulting increased radial gradient of  $|B|_{0,0}$  improves the confinement of energetic trapped particles by increasing their poloidal drift, analogous to the way that the ambipolar electric field improves the confinement of thermal particle orbits [13]. A consequence of this is that alpha particle confinement improves with increasing  $\beta$  [5]. At  $\beta = 23\%$ , the level of alpha energy losses is  $\sim 12\%$ .

In summary, we have found compact, quasipoloidally symmetric stellarators with high MHD stability  $\beta$  limits and good neoclassical confinement. The rotational transform in these hybrid configurations is produced primarily by a self-consistent bootstrap current. The nonaxisymmetric components of  $|B|$  yield a bootstrap current lower than that in an axisymmetric device, which leads to good MHD stability properties without the need for a conducting wall. The neoclassical confinement improves with increasing  $\beta$ , leading to a new form of configurational invariance in these stellarators.

The authors thank D. B. Batchelor, D. Strickler, and M. B. Nestor for comments and suggestions. This research was supported by the U.S. Department of Energy under Grant No. DE-FG 03-97ER54423 at the University of Montana and under Contract No. DE-AC05-00OR22725 at Oak Ridge National Laboratory, managed by UT-Battelle, LLC.

- 
- [1] G. Grieger *et al.*, *Plasma Physics and Controlled Nuclear Fusion Research, Proceedings of the 13th International Conference, Washington, 1990* (International Atomic Energy Agency, Vienna, 1991), Vol. 3, p. 525.
  - [2] S. P. Hirshman *et al.*, *Phys. Plasmas* **6**, 1858 (1999).
  - [3] D. T. Anderson *et al.*, *J. Plasma Fusion Res.* **1**, 49 (1998).
  - [4] G. H. Neilson *et al.*, *Phys. Plasmas* **7**, 1911 (2000).
  - [5] D. A. Spong *et al.*, *Nucl. Fusion* **41**, 711 (2001).
  - [6] A. H. Boozer, *Phys. Fluids* **23**, 904 (1980).
  - [7] K. C. Shaing *et al.*, *Phys. Fluids B* **1**, 148 (1989).
  - [8] W. I. van Rij and S. P. Hirshman, *Phys. Fluids B* **1**, 563 (1989).
  - [9] R. Sanchez *et al.*, *J. Comput. Phys.* **161**, 576 (2000).
  - [10] W. A. Cooper, D. B. Singleton, and R. L. Dewar, *Phys. Plasmas* **3**, 275 (1996).
  - [11] G. Y. Fu, *Phys. Plasmas* **7**, 1079 (2000).
  - [12] U. Stroth *et al.*, *Nucl. Fusion* **36**, 1063 (1996).
  - [13] M. Yokoyama *et al.*, *Nucl. Fusion* **40**, 261 (2000).